Asociación Argentina de Mecánica Computacional

Mecánica Computacional Vol XXXIII, págs. 2371-2385 (artículo completo)
Graciela Bertolino, Mariano Cantero, Mario Storti y Federico Teruel (Eds.)
San Carlos de Bariloche, 23-26 Setiembre 2014

NEW FORMULATION FOR CHAOTIC INTERMITTENCY WITHOUT NOISE

Sergio Elaskar[a,b,d], Ezequiel del Río[c] and Gustavo Krause[a,b]

[a] *Departamento de Aeronáutica, Universidad Nacional de Córdoba, Av. Velez Sarfield 1611, 5000 Córdoba, Argentina*

[b] *CONICET*

[c] *Departmento de Física Aplicada, ETSIA, Universidad Politécnica de Madrid, Plaza Cardenal Cisneros 3, Madrid, Spain*

[d] *sergio.elaskar@gmail.com*

Keywords: Intermittency, Chaos.

Abstract. The proper description of turbulent flows presents difficulty for researchers in fluid mechanics. One feature of some of these flows is intermittency. The intermittency phenomenon in Chaotic Dynamics theory is understood as a specific route to the deterministic chaos when spontaneous transitions between laminar and chaotic dynamics occur. A correct characterization of the intermittency is important, principally, to study those problems having partially unknown governing equations or there are experimental or numerical data series. This paper presents a review of a new methodology to investigate systems showing chaotic intermittency phenomenon without noise is presented. To evaluate the statistical properties of the chaotic intermittency a theoretical RPD is obtained. This function depends on two parameters, the lower bound of reinjection and an exponent which describes the non-linear reinjection processes. Once evaluated the RPD function, other properties such as the probability of the laminar length and the characteristic relation are obtained. The key of the new formulation is the introduction of a new function, called M(x), which is utilized to calculate the RPD function in place to consider the huge number of numerical or experimental data. The function M(x) depends on two integrals, this characteristic reduces the influence on the statistical fluctuations in the data series. Also, the function M(x) is easy to evaluate. With this new approach, more accurate analytical expressions for the intermittency statistical properties are obtained. And, it is shown that the behavior of the intermittency phenomena is more rich and complex that those given by the classical theory used until now. On the other hand, the new analytical RPD function is more general than the previous ones; and the classical uniform reinjection is only a particular case.

1 INTRODUCTION

Intermittency is a particular route to chaos, where a transition between regular or laminar and chaotic phases occur. Pomeau and Maneville introduced the concept of intermittency in (Manneville and Pomeau, 1979) and it has been observed in several fluid dynamics topics such as plasma physics and derivative non-linear Schrodinger equation (Sanmartín et al., 2004; Sanchez-Arriaga et al., 2007); Lorenz system (Manneville and Pomeau, 1979); Rayleigh-Bénard convection (Dubois et al., 1983) and turbulence (Manneville, 2004), etc. Therefore, it is very important to properly characterise the intermittency phenomenon.

Traditionally, intermittency is calssified into three differents types called I, II and III (Schuster and Wolfram, 2005; Nayfeh and Balachandran, 1995) according to the Floquet multipliers or eigenvalue in the local Poincaré map. In intermittency type-I one of the Floquet multipliers leaves the unit circle through +1, there is a tangent bifurcation (Nayfeh and Balachandran, 1995). Intermittency type-II begins in a subcritical Hopf bifurcation or Naimark-Sacker bifurcation (Wiggins, 1990), therefore, two complex-conjugate Floquet multipliers or two complex-conjugate eigenvalues of the local Poincaré map exit the unit circle. Type-III intermittency is related to a subcritical period-doubling or flip bifurcation when one Floquet multiplier leaves the unit circle through -1. In the intermittency phenomenon, when a control parameter exceeds a threshold value, the system behaviour changes abruptly to a larger attractor by means an explosive bifurcation (Nayfeh and Balachandran, 1995). Then, the periodic orbit becames chaotic.

By means of Poincaré sections it is possible to study the intermittency mechanism using maps. In all the cases, a fixed point of the local Poincaré map becomes unstable for positive values of a control parameter ε. The local Poincaré maps for type-I, type-II and type-III intermittencies are respectively given by: $x_{n+1} = \varepsilon + x_n + a\ x_n^2$, $x_{n+1} = (1+\varepsilon)x_n + a\ x_n^3$ and $x_{n+1} = -(1+\varepsilon)\ x_n - a\ x_n^3$, where ε and a must be higher than 0. However, to generate intermittency it is necessary to have a reinjection mechanism that maps back from the chaotic zone into the local regular or laminar one. This mechanism is described by the reinjection probability density function (RPD), which is determined by the non linear dynamics of the system itself. Therefore, the accurate evaluation of the RPD function is extremely important to correctly analize and describe the intermittency phenomenon. It is important to note that in only a few cases it is possible to obtain an analytical expression for the RPD function. Also, it is not a simple task to experimentally or numerically obtain the RPD due to the huge amount of data needed; and the statistical fluctuations induced in the numerical computations and the experimental measurements are difficult to be estimated. For theses reasons several different approaches have been used to describe the RPD for the intermittent systems. The most implemented approach considers the RPD as a constant; therefore, there is uniform reinjection. However, specific approaches have been utilized, which are built using a characteristic of the particular non-linear proccesses. Nevertheless, these RPD functions can not be applied for other systems. An example is given by (Kye and Kim, 2000) to investigate the effect of noise in type-I intermittency. They assumes that the reinjection is concentrated in a fixed point.

There was not an efficient method to obtain the RPD function. However, recently a more general RPD that includes the uniform reinjection as a particular case had been introduced (del Río and Elaskar, 2010; Elaskar et al., 2011; del Río et al., 2012; Elaskar and del Río, 2012; del Río et al., 2013, 2014; Krause et al., 2014a,b). In this paper we present a complete description of the new formulation for type-I, II and III intermittencies. The formulation includes the lower bound of the reinjection (LBR), and permits the other statistical variables calculation, such as the probability of the laminar length and the characteristic relations.

2 FORMULATION FOR THE RPD FUNCTION

We consider a general one-dimensional map: $x_{n+1} = F(x_n)$. The RPD function, called here by $\phi(x)$, gives the statistical behavior of the reinjection trajectories, and it depends on the specific form of $F(x)$. The main concept to reach a more general formulation is given by the following integral (del Río et al., 2012):

$$M(x) = \begin{cases} \frac{\int_{\hat{x}}^{x} \tau\, \phi(\tau)\, d\tau}{\int_{\hat{x}}^{x} \phi(\tau)\, d\tau} & \text{if } \int_{\hat{x}}^{x} \phi(\tau) d\tau \neq 0 \\ 0 & \text{otherwise} \end{cases} \tag{1}$$

Where $\hat{x}$ and c are the lower boundary of reinjection and the end of the laminar zone around of the unstable fixed point x_0 respectivelly. $\hat{x}$ can be lower, iqual or higher than zero. However, c is a constant verifying $c > 0$; and always the inequality $\hat{x} \leq x \leq c$ must be verify. Then, the laminar interval is defined by $[\hat{x}; x_0 + c]$. In the previous work (del Río and Elaskar, 2010) we used $\hat{x} = x_0$; however, a more general approach considering $\hat{x}$ different to x_0 was established in (Elaskar et al., 2011). Note that the integral $M(x)$ smooths the experimental o numerical data series, and its numerical estimation is more robust than the direct evaluation of the RPD function, $\phi(x)$. Also, the practical evaluation of the function $M(x)$ is very simple, we can calculate it as:

$$M(x) \approx \frac{1}{n} \sum_{j=1}^{n} x_j, \qquad x_{n-1} < x \leq x_n \tag{2}$$

where the reinjection points $\{x_j\}_{j=1}^{N}$ must be sorted from lowest to highest, i.e. $x_j \leq x_{j+1}$. We found that for a wide class of maps exhibiting intermittency, the function $M(x)$ satisfies a linear approximation:

$$M(x) = \begin{cases} m(x - \hat{x}) + \hat{x} & \text{if } \ x \geq \hat{x} \\ 0 & \text{otherwise} \end{cases} \tag{3}$$

where the slope $m \in (0, 1)$ is a free parameter. Then, using Eqs.(1 and 3) we can obtain the corresponding RPD:

$$\phi(x) = \lambda(x - \hat{x})^{\alpha}, \quad \text{with} \quad \alpha = \frac{2m - 1}{1 - m} \tag{4}$$

where λ is a normalization constant and $\alpha > -1$ becuase $0 < m \leq 1$. Note that for $m = 1/2$ we recover the uniform RPD, $\phi(x) = cte$. Therefore, the new formulation is more general, and it includes the uniform reinjection as a particular case.

3 TYPE-I INTERMITTENCY

We use a quadratic map to represent the local map for type-I intermittency:

$$x_{n+1} = f(x) = a x_n^2 + x_n + \varepsilon, \tag{5}$$

where ε is the control parameter and it represents the channel width in the laminar region, i.e. the distance between the local Poincaré map and the bisectrix. The parameter a specifies the position of the point with zero-derivative. In the last equation, for $\varepsilon < 0$ there are two fixed point, one of them stable and other one unstable. For $\varepsilon = 0$ the two fixed points coalesce in one fixed point $x_0 = 0$; and for $\varepsilon > 0$ there are not fixed points. Furthermore, if there is a reinjection mechanims mapped back from the chaotic zone into the local one, type-I intermittency can exist.

The map implmented by (del Río et al., 2013) is used. For that map the non-linear reinjection mechanims is given by: $g(x) = \hat{x} + h(x - x_r)^\gamma$. The coefficient h is obtained from $g(x_r) = \hat{x}$ and $g(1) = 1$. We consider that the LBR is placed inside of the laminar intervalm then $|\hat{x}| \leq c$.

The global map can be written as:

$$\begin{array}{ll} F(x) = f(x) = ax^2 + x + \varepsilon, & x < x_r, \\ F(x) = g(x) = \hat{x} + \frac{f(x_r) - \hat{x}}{(f(x_r) - \hat{x})^\gamma}(x - \hat{x})^\gamma & x > x_r \end{array} . \tag{6}$$

The exponent γ permits to obtain differents RPD functions. For $\gamma > 1$ the trajectories are concentrated around the LBR point, therefore the RPD has a decreasing structure. However, for $0 < \gamma < 1$ the trajectories move away from the LBR point, then the RPD function has an increasing form. For $\gamma = 1$, the RPD is approximatelly uniform.

Figure 1 shows the map (6) for three different values of the exponent γ.

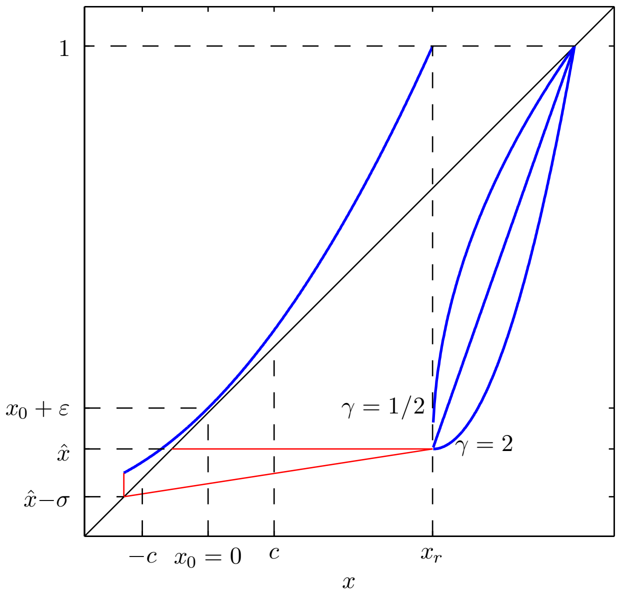

Figure 1: Map $F(x)$ given by Eq. (6) for different values of the exponent γ. The LBR produced bay the noise effect is indicated too.

In this work, to obtain the RPD, the theoretical methodology developed by (del Río and Elaskar, 2010; Elaskar et al., 2011; del Río et al., 2014) is extended. The RPD function is evaluated from the function $M(x)$ which is obtained from numerical or experimental data. The function $M(x)$ is defined inside of the laminar interval $[-c, c]$ using Eq.(2). Note that $M(x)$ is an average over the reinjection points in the laminar interval, and its evaluation is easier than the direct RPD calculation.

For a wide class of maps exhibiting type-I intermittency without considering noise, the function $M(x)$ satisfies a linear approximation if the LBR is placed inside of the laminar interval ($-c < \hat{x} < c$) (Krause et al., 2014a). Therefore, the RPD function is given by Eq.(4).

The laminar length counts the number of iterations spent by the trajectory inside of the laminar interval, and it depends only on the local map. However, the probability of the laminar length function, $\phi_l(l)$ takes in consideration the reinjection mechanims. $\phi_l(l)$ determines the probability to find an specific laminar length.

The local Poincaré map given by Eq.(5) is used to evaluate the laminar length. If we consider $\epsilon \to 0$, the difference $x_{n+1} - x_n$ can be approximated by the following differential equation (Schuster and Wolfram, 2005):

$$\frac{dx}{dl} = ax^2 + \varepsilon, \tag{7}$$

The solution of the last equation inside of the interval $[-c, c]$ results:

$$l(x,c) = \int \frac{1}{ax^2+\varepsilon} dx = \frac{1}{\sqrt{a\varepsilon}}[\tan^{-1}(\sqrt{\frac{a}{\varepsilon}}c) - \tan^{-1}(\sqrt{\frac{a}{\varepsilon}}x)]. \tag{8}$$

Then, for type-I intermittency, the probability to find a laminar length between l and $l + dl$ is (Schuster and Wolfram, 2005):

$$\phi_l(l) = \phi[X(l,c)] \left| \frac{dX(l,c)}{dl} | = \phi[X(l,c)] | a[X(l,c)\right]^2 + \varepsilon|, \tag{9}$$

where $X(l, c)$ is the inverse function of $l(x, c)$ given by Eq.(8):

$$X(l,c) = \sqrt{\frac{\varepsilon}{a}} \tan[\tan^{-1}(\sqrt{\frac{a}{\varepsilon}}c) - \sqrt{a\varepsilon}l]. \tag{10}$$

Note that the characteristics of the function $\phi_l(l)$ depend on the LBR and α. Figure 2 shows the different form for the probability of the laminar length in type-I intermittency (del Río et al., 2014)

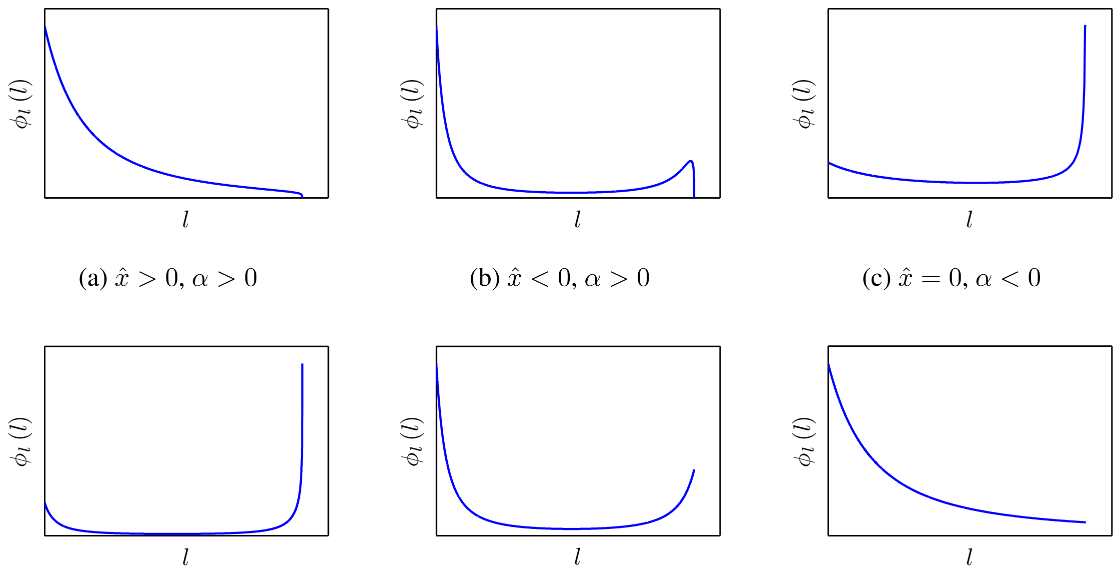

(a) $\hat{x} > 0, \alpha > 0$ (b) $\hat{x} < 0, \alpha > 0$ (c) $\hat{x} = 0, \alpha < 0$

(d) $\hat{x} < 0, \hat{x} < 0$ (d) $\hat{x} < 0, \alpha = 0$ (f) $\hat{x} > 0, \alpha = 0$

Figure 2: Probability of the laminar length, $\phi_l(l)$, for several LBR and α

4 TYPE-II INTERMITTENCY

In this section we applied the new formulation to an illustrating one-dimensional map presenting type-II intermittency (del Río and Elaskar, 2010):

$$x_{n+1} = \begin{cases} F(x_n) & x_n \le x_r \\ (F(x_n)-1)^{\gamma} & x_n > x_r \end{cases} \tag{11}$$

where $F(x) = (1+\varepsilon)x_n + (1-\varepsilon)x_n^p$, x_r is defined by $F(x_r) = 1$, and ε is the control parameter. The origin of the map $x = 0$ is always a fixed point, however it is only stable for $-2 < \varepsilon < 0$. For $\varepsilon > 0$ the fixed point is unstable. The iterated points x_n of an inicial point, close to the origin, increases due to a process governed by parameters ε and p. A chaotic burst happens if x_n becomes larger than x_r; this chaotic process will be finished when x_n is reinjected into the laminar zone. From this reinjected point, a new iterative process again governed by ε and p will cause an increase of the iterative points. Note that γ drives the reinjection mechanism, whereas p and ε influence the laminar phase duration. If we consider $\gamma = 1$ and $p = 2$ in Eq.(11), we recover the map used by Manneville in his pioneer paper (Manneville and Pomeau, 1979). If we use $p = 3$, the local form of the map represents the local Poincaré map of type-II intermittency.

We have numerically evaluated the function $M(x)$ obtaining, in approximation, the following linear form $M(x) = mx$. Figure 3 shows numerical evaluations of $M(x)$ for different values of parameter γ together with the corresponding least squares straight line fitting. Always we find that $|m| < 1$. We have used the following parameters: in the upper line $\gamma = 2$ and $\varepsilon = 10^{-3}$, and for the lower line $\gamma = 0.65$ and $\varepsilon = 10^{-4}$. According to previous results, we consider that the function M is linear, $M(x) = mx$. Then the RPD can be expressed by Eq.(4) with $\lambda = \frac{\alpha+1}{c^{\alpha+1}}$. Note that $\phi(x)$ is determined only by the parameter m, which is easier to measure than the complete function $\phi(x)$. Note that the shape of $\phi(x)$ can be very different from the flat line (uniform reinjection), for instance $\lim_{x\to 0}\phi(x)$ is infinity when $0 < m < 1/2$ and zero if $1/2 < m < 1$. In Figure 4 points indicate the numerical RPD functions, and the theoretical functions for $\phi(x)$ given by Eq.(4) are represented by continuous lines. We are considering the same two cases shown in Fig.(3). We can observe that the numerical data and theoretical results have a very good agreement. Note that the continuous curve reduces the statistical fluctations of the numerical data. We observe that the slope m determines the value of the exponent α in the reinjection function (4), hence it rules the reinjection mechanism and it has direct influence in the the length probability density, the average laminar length and the characteristic relation. The density of the laminar lengths probability $\phi_l(l)$ is a global property and it is related to $\phi(l, c)$

$$\phi_l(l,c) = \lambda \left(\frac{\varepsilon}{\left(a + \frac{\varepsilon}{c^{(p-1)}}\right) e^{(p-1)\varepsilon l} - a} \right)^{\frac{p+\alpha}{p-1}} \times \\ \times \left(a + \frac{\varepsilon}{c^{(p-1)}}\right) e^{(p-1)\varepsilon l} \tag{12}$$

We can note that $\phi_l(l, c)$ depends on the global parameter α. Hence, the probability of the laminar length is determined by the slope m of the function $M(x)$. Fig.(5) shows a comparisson between the analytical results calculated using Eq.(12) with the numerical results for the map (11). We can observe a good agreement between numerical data and the theoretical results. Another important property of the intermittent behaviour is the average laminar length $\bar{l}$, that if m does not depend on ε, can be written as del Río and Elaskar (2010):

$$\bar{l} \approx \frac{1}{ac^{\alpha+1}} \left(\frac{a}{\varepsilon}\right)^{\frac{p-\alpha-2}{p-1}} \frac{\pi}{p-1} \sin^{-1}\left(\frac{\pi(1+\alpha)}{p-1}\right) \tag{13}$$

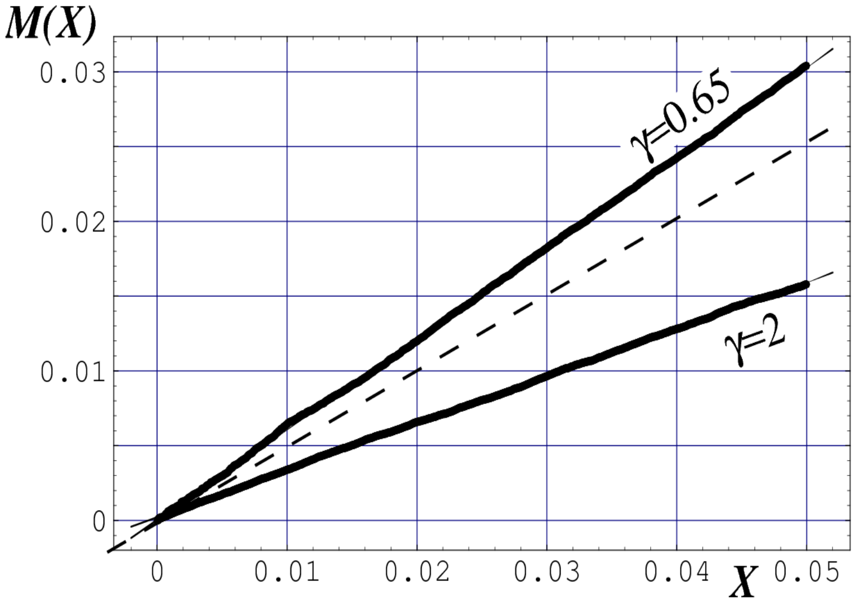

Figure 3: Function $M(x)$ for the map (11) with $p = 3$. Continuous lines show the linear fit of the numerical data. The slope of the dashed line is 0.5. In the upper line $\gamma = 2$ and $\varepsilon = 10^{-3}$ whereas for the lower case $\gamma = 0.65$ and $\varepsilon = 10^{-4}$

so the characteristic relation can be writte as:

$$\bar{l} \propto \varepsilon^{\frac{\alpha+2-p}{p-1}} \tag{14}$$

The characteristic relation depends on both: the behavior of the local map around the fixed point, and on the global dynamic of the map represented by the parameters α or m. The map (11), in the region where the chaotic dynamic occurs, depends on the exponent γ, so we expect that the RPD also will depend on γ. Then, we expect that α and m will be strongly dependent on γ and weakly on parameters ε.

5 TYPE-III INTERMITTENCY

Dubios and co-authors found type-III intermittency in the Bénard convection in a rectangular cell; and they presented a Poincaré map without reinjection around the neighborhood of the unstable fixed point (Dubois et al., 1983). This behavior suggests that exists a lower bound of the reinjection. In this section, we will extend the results obtained in the previous sections to type-III intermittency to reach a complete description of the laminar length statistic and the effect of the LBR. To do this we will use the function $M(x)$ following (Elaskar et al., 2011).

We introduce an illustrating map:

$$\begin{aligned} x_{n+1} = F(x_n) = -(1+\varepsilon)\, x_n - a\, x_n^3 + \\ + b\, x_n^6\, \sin(x_n) \quad \text{with} \quad a > 0 \end{aligned} \tag{15}$$

where $x = 0$ is a fixed point of the map. This fixed point is asymptotically stable when ε satisfies $-2 < \varepsilon < 0$, and it is unstable for $\varepsilon > 0$ and the Schwartzian derivative *SF*(x) is positive. The last term in Eq.(15) provides an efficient mechanism for reinjection. The non-linear behavior of the Eq.(15) is completely different from the non-linear behavior of the maps used for type-I and

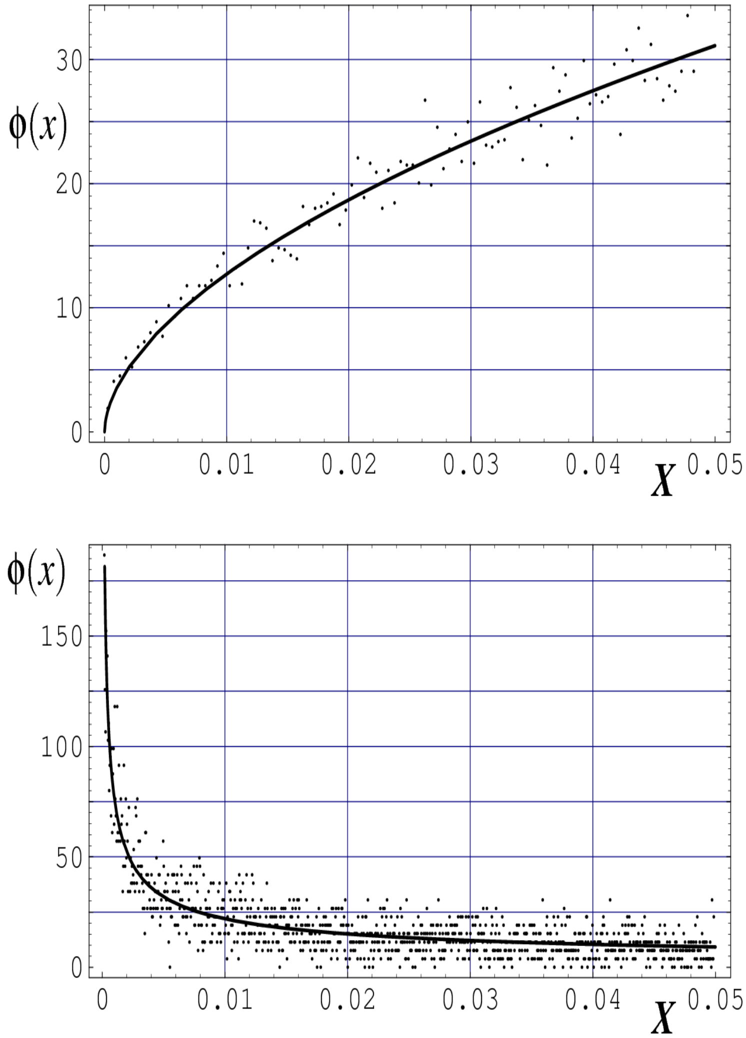

Figure 4: RPD for map (11). Upper and lower pictures correspond with the upper and lower lines of Fig.(3) respectively. Dots indicate numerical evaluations and continuous lines show the analytival results.

II intermittencies. Therefore, with the map (15) we not only study type-III intermittency, but we also extend the new formulation to another wide set of maps. The reinjection mechanism depends on the value of $F(x_r)$ at extreme points x_r. As n increases, any point x_n close to the origin evolves in a process govern by the parameters ε and a. For enough large n, the RHS third term effect in Eq.(15) increases and x_n approaches a x_r point giving rise the reinjection mechanism into the laminar zone. We note thta there is no reinjection around the unstable fixed point for $b > b_c \simeq 1.07$ (Elaskar et al., 2011). However, there is not LBR if $b < b_c$ for the same values of a and ε. The map is shown in Figure 6.

Figure 7 plots the function $M(x)$ of Eq.(15) for $a = 1$ and $\varepsilon = 0.01$. There are two functions $M(x)$ calculated using two different values of the parameter b which can be approximated by straight lines, hence according with Eq.(3) we get m and by setting $M(\hat{x}) = \hat{x}$ we can obtain the LBR value $\hat{x}$. Hence by reinjection probability density function can be described by Eq.(4), where $\lambda = \frac{1}{2}\frac{\alpha+1}{(c-\hat{x})^{\alpha+1}}$.

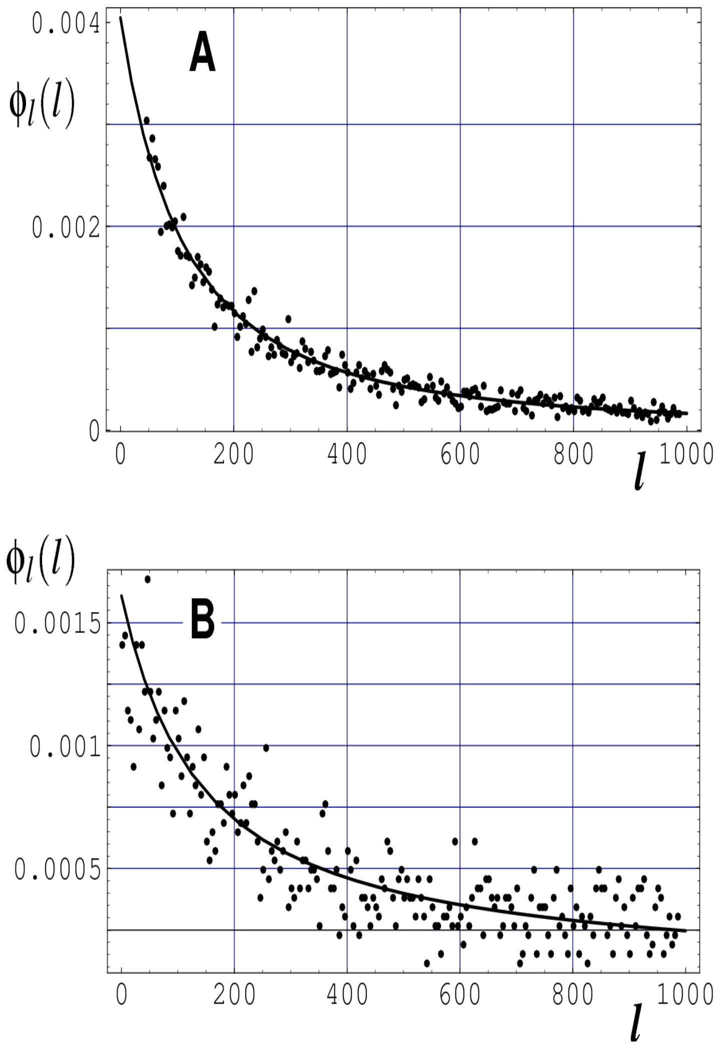

Figure 5: ϕ_l for map (11) using the same parametres that as Fig.(3).

For Fig.(7), we found that $m = 0.36$ and $m = 0.37$ for the lower and upper line respectively. Fig.(8) shows the RPD functions for the same tests indicated in Fig.(7). The continuous curve represents the analytical expression given by Eq.(3). Note that the agreement between theoretical results and numerical data is very good. A LBR different from zero produces a gap around the unstable point in the Poincaré map ($\hat{x} \neq 0$). The LBR appears in the function $\phi(x) = \lambda x^\alpha$ as a positive shift on the variable x. Also, negative values of $\hat{x}$ can also be possible for Eq.(4). Therefore, if $\hat{x} < 0$, the RPD function can be described by two overlapping functions, each one having the form given by Eq.(4):

$$\phi(x) = \begin{array}{l} \lambda[(|\hat{x}| + x)^\alpha + (|\hat{x}| - x)^\alpha] \text{ if } |x| - |\hat{x}| \\ \lambda(|\hat{x}| + x)^\alpha \text{ if } |\hat{x}| < x - c \\ \lambda(|\hat{x}| - x)^\alpha \text{ if } -c < x - |\hat{x}| \end{array} \qquad (16)$$

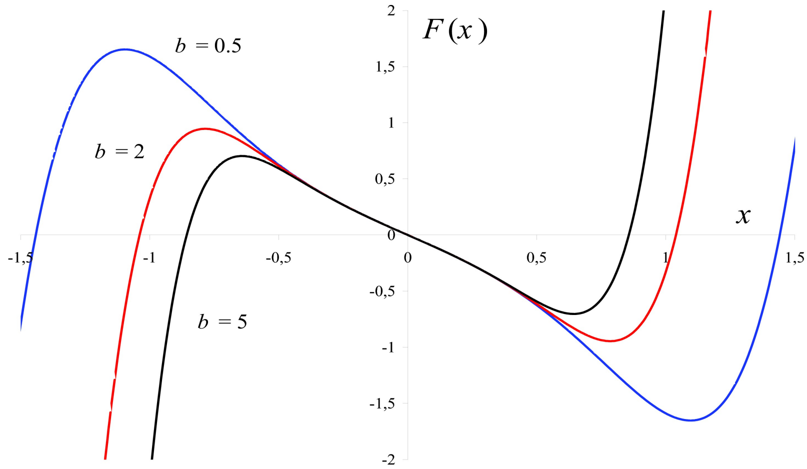

Figure 6: Map for diffrent values of b.

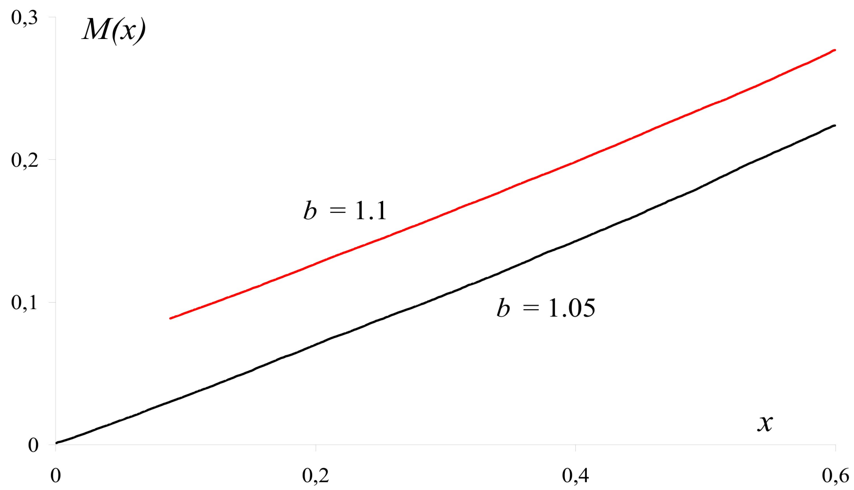

Figure 7: Numerical function $M(x)$ for the map (15). For the lower line $b = 1.05$ and for upper one $b = 1.1$. After numerical fitting, we obtain $m \approx 0.36$, $\hat{x} \approx 0$ and $m \approx 0.37$, $\hat{x} \approx 0.053$, respectively. The rest of the parameters used are $a = 1$ and $\varepsilon = 0.01$.

where $\lambda > 0$ is again a normalization parameter

$$\lambda = \frac{1}{2} \frac{\alpha + 1}{(c + |\hat{x}|)^{\alpha+1}} \tag{17}$$

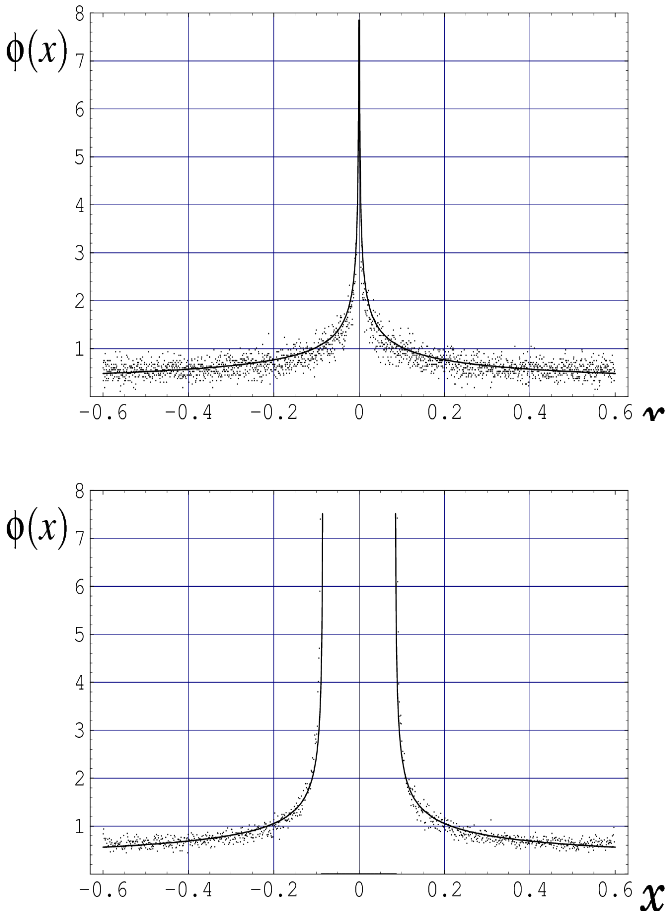

Figure 8: RPD for the same parameters used for Fig.(7). Dots are numerical data and continuous lines represent the Eq.(4).

The RPD given by Eq.(16) is also specified by the two parameters α and $\hat{x}$, as in the previous case. However, the function $M(x)$ is not linear in x because the reinjection mechanism is produced by superimposing two simultaneous processes (see Fig.9). The RPD given by Eq.(16) is non-continuous for $x = |\hat{x}|$, then $M(x)$ has no derivative at this point. Therefore, the point $\hat{x}$ is a singular point for both $M(x)$ and $\phi(x)$. To obtain the expression for $M(x)$ we use Eqs.(3) and (16):

$$M(x) = \frac{(1+\alpha)\,x - |\hat{x}|}{(2+\alpha)} \left[\frac{|\hat{x}|\,(|\hat{x}|-x)^{1+\alpha} - |\hat{x}|^{2+\alpha}}{(|\hat{x}|-x)^{1+\alpha} - (|\hat{x}|+x)^{1+\alpha}}\right] \frac{2}{(2+\alpha)} \tag{18}$$

To calculate α we evaluate the Eq.(18) for $x = |\hat{x}|$. To verify the assumptions made in obtaining the RPD in Eq.(16), we compare numerical data for $M(x)$ with Eq.(18). In Fig.(9) we plot both analytical and numerical M. In Fig.(10) we compare the RPD function, Eq.(16), with the numerical data. The values of $\hat{x}$ and α have been calculated from the function $M(x)$ for the same parameters used in Fig.(9). The overlapping of the function $\phi(x)$ is clearly exhibited in the figures. Once the RPD function is calculated, it is possible to evaluate the laminar length,

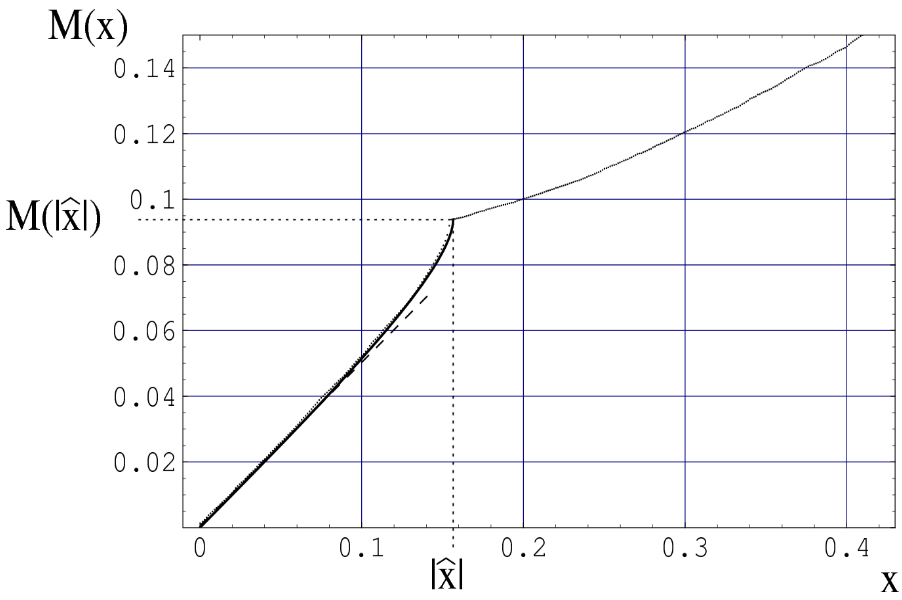

Figure 9: Numerical evaluation of $M(x)$. Singular point is $|\hat{x}| \approx 0.157$. The continuous line represents Eq.(18) for $x < |\hat{x}|$ and the dashed one is the straight line with slope 1/2. The parameters are $a = 1.035$, $b = 1.05$ and $\varepsilon = 0.001$.

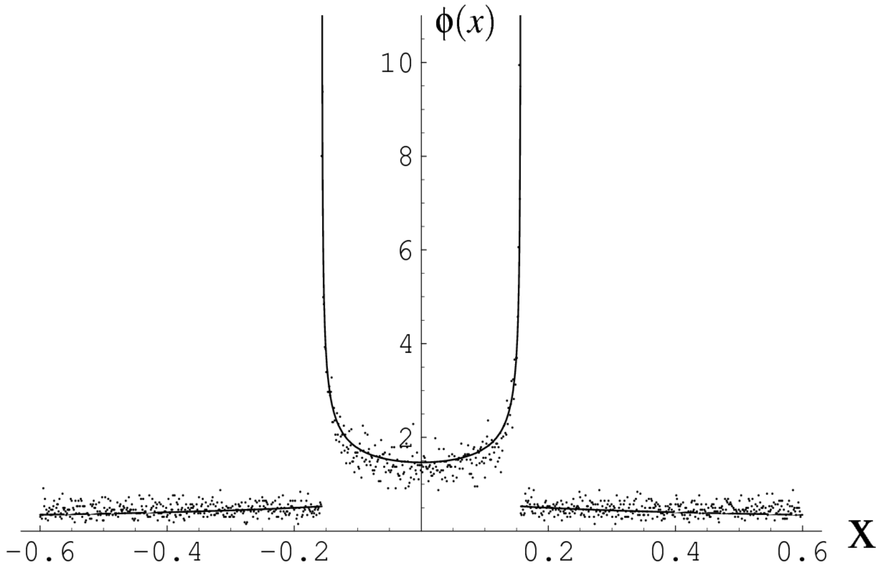

Figure 10: RPD for the same parameters used in Fig.(9). Dots are numerical data and continuous lines are referred Eq.(16).

and their probability density

$$\phi_l(l) = 2\lambda \left(X(l,c) - \hat{x}\right)^{\alpha} \left[aX(l,c)^3 + \varepsilon X(l,c)\right] \tag{19}$$

where $X(l,c) = \sqrt{\frac{\varepsilon}{(a+\varepsilon/c^2)e^{2\varepsilon\, l} - a}}$.

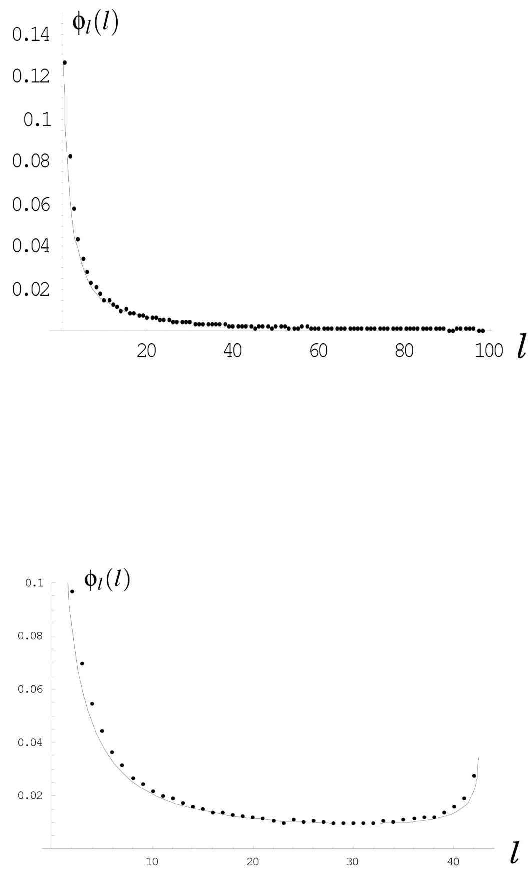

Figure 11: ϕ_l for the same test of Fig.(9). Eq.(19) is represented by lines.

Fig.(11) shows the comparison between numerical data for the probability density of laminar length and the results calculated with Eq.(19). To obtain this figure we have used the same parameters $\hat{x}$ and m corresponding to lower and upper line respectively of Fig.(7). Note that in Fig.(11.a) the probability of laminar phase length values can be arbitrarily very large because of $\hat{x} \approx 0$. On the contrary, for $b = 1.1$, we have $\hat{x} > 0$ and this fact gives rise the existence of an upper cut-off value, $\hat{l}$, as shown in Fig.(11.b). For $\hat{x} < 0$, by ussing Eqs.(16) and (19), the probability density of the laminar length can be written as:

$$\begin{aligned}\phi_l(l) = 2\lambda\left[(|\hat{x}| + X(l,c))^{\alpha} + +k\left(|\hat{x}| - X(l,c)\right)^{\alpha}\right] \\ \left[aX(l,c)^3 + \varepsilon X(l,c)\right]\end{aligned} \tag{20}$$

where $k = 0$ for $|l| \leq \left|\hat{l}\right|$ and $k = 1$ for $|l| > \left|\hat{l}\right|$.

Fig.(12) shows the comparison between the numerical values and the Eq.(20). The parameters $\hat{x}$, α and λ used in this figure are the same that we used in Figs.(9 and 10). When $\hat{x} > 0$ we find that $\hat{l}$ is a cut-off value, whereas for $\hat{x} < 0$ the function ϕ_l does not have a cut-off and this function continues to infinite.

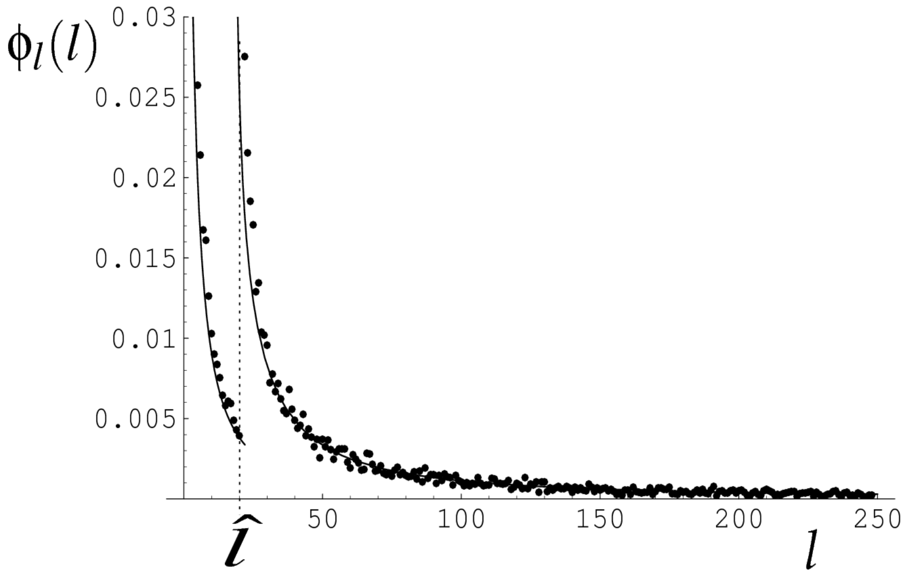

Figure 12: ϕ_l for the same test of Fig.(10). Eq.(20) is represented by lines.

6 CONCLUSIONS

In this paper we have presented a review about of a new formulation for chaotic intermittency. This formulation is general and we have applied to type I, II and III intermittencies with and without LBR. The methodology is based on a new function, called $M(x)$, and with this function we can calculate the RPD function for a broad class of systems.

The function $M(x)$ is easy to calculate; and it has a linear form for several maps. Also, by means of a numerical evaluation of the function $M(x)$, we have obtained the values of the parameters m and $\hat{x}$. With only theses two parameters, we provide a whole description of the RPD function. Once we have obtained the RPD function, we can establish new analytical relations for the probability density of the laminar length.

When $\hat{x} > 0$, the system has a LBR and there is a cut-off value for the probability of the laminar lengths. For $\hat{x} < 0$ the system has a more complex RPD which is a linear combination of RPD describing the case of $\hat{x} > 0$. This behavior modified the linearity of the function $M(x)$. However, even in these tests, the function $M(x)$ provides us enough information to completely determine the function $\phi(x)$.

We have found more complex RPD functions that those generated by uniform reinjection; and the uniform reinjection is only an specific case in the new theory. The same applies for the probability of the laminar lengths. For example, for type I intermittency we have obtained several probabilities of the laminar length as function of the LBR and the exponent α

Finally, we highlight that in all performed tests, the numerical data and theoretical results have shown a very good agreement.

REFERENCES

del Río E. and Elaskar S. New characteristic relation in type-ii intermittency. *International Journal of Bifurcation and Chaos*, 20:1185–1191, 2010.

del Río E., Elaskar S., and Donoso J. Laminar length and characteristic relation in type-i intermittency. 19:967–976, 2014.

del Río E., Elaskar S., and Makarov V. Theory of intermittency applied to classical pathological cases. *Chaos*, 23:033112, 2013.

del Río E., Sanjuan M., and Elaskar S. Effect of noise on the reinjection probability density in intermittency. *Comunication in Nonlinear Sciences and Numerical Simulation*, 17:3587–3596, 2012.

Dubois M., Rubio M., and Berge O. Experimental evidence of intermittencies associated with a subharmonic bifurcation. 51:1446–1449, 1983.

Elaskar S. and del Río E. Intermittency reinjection probability function with and without noise effects. *Latest Trends in Circuits, Automatics Control and Signal Processing*, 1:145–154, 2012.

Elaskar S., S. del Río E., and Donoso J. Reinjection probability density in type-iii intermittency. *Physica A*, 390:2759–2768, 2011.

Krause G., Elaskar S., and del Río E. Noise effect on statistical properties of type-i intermittency. *Physica A*, 402:318–329, 2014a.

Krause G., Elaskar S., and del Río E. Type-i intermittency with discontinuous reinjection probability density in a truncation model of the derivative nonlinear schrÃűdinger equation. *Physical Review Letter*, 2014b.

Kye W. and Kim C. Cha. *Physical Review E*, 62:6304–6307, 2000.

Manneville P. *Instabilities, Chaos and Turbulence.* Imperial College Press, 2004.

Manneville P. and Pomeau Y. Intermittency and lorenz system. *Physics Letter A*, 75:1–2, 1979.

Nayfeh A. and Balachandran B. *Applied Nonlinear Dynamics.* John Wiley, 1995.

Sanchez-Arriaga G., Sanmartín J., and Elaskar S. Damping models in the truncated dnls equation. *Physics of Plasmas*, 14:082108, 2007.

Sanmartín J., López-Rebollal O., del Río E., and Elaskar S. Hard transition to chaotic dynamics in alfvén wave-fronts. *Physics of Plasmas*, 11:2026–2035, 2004.

Schuster H. and Wolfram J. *Deterministic Chaos.* WILEY-VCH Verlag GmbH, 2005.

Wiggins S. *Introduction to Applied Nonlinear Dynamical Systems and Chaos.* Springer-Verlag, 1990.